Journal of Advanced Ceramics
2014, 3(2): 147–154
DOI: 10.1007/s40145-014-0105-1

ISSN 2226-4108
CN 10-1154/TQ

Research Article

Microstructure and piezoelectric properties of $K_{5.70}Li_{4.07}Nb_{10.23}O_{30}$-added $K_{0.5}Na_{0.5}NbO_3$ ceramics

Xuming PANG[b], Jinhao QIU[a,*], Kongjun ZHU[a]

[a]*State Key Laboratory of Mechanics and Control of Mechanical Structures*, *Nanjing University of Aeronautics and Astronautics*, *Nanjing 210016*, *China*
[b]*Department of Mechanical Engineering*, *Nanjing Tech University*, *Nanjing 210009*, *China*

Received: January 19, 2014; Revised: March 26, 2014; Accepted: April 12, 2014

Abstract: Lead-free piezoelectric ceramics $K_{0.5}Na_{0.5}NbO_3$–*x*mol%$K_{5.70}Li_{4.07}Nb_{10.23}O_{30}$ (x = 0–2.5, KNN–*x*mol%KLN) were prepared by conventional sintering technique. The phase structure and electrical properties of KNN ceramics were investigated as a function of KLN concentration. The results showed that small amount of KLN introduced into the lattice formed a single phase perovskite structure. The KLN modification lowered the phase transition temperature of orthorhombic–tetragonal ($T_{O–T}$) and increased the Curie temperature (T_C). Some abnormal coarse grains were formed in a matrix when the content of KLN was relatively low (1 mol%). However, normally grown grains were only observed when the sintering aid content was increased to 2 mol%. Proper content of KLN decreased the amount of defects, thus the remanent polarization increased and the coercive field decreased markedly, and the sinterability of the KNN ceramics was simultaneously improved with significant increase of piezoelectric properties.

Keywords: ceramics; sintering aid; phase transformation; electrical properties

1 Introduction

Lead-based ferroelectric materials, such as $Pb(Zr,Ti)O_3$ (PZT), $Pb(Mg_{1/3}Nb_{2/3})O_3$–$PbTiO_3$ (PMN–PT) and $Pb(Zn_{1/3}Nb_{2/3})O_3$–$PbTiO_3$ (PZN–PT), show excellent piezoelectric properties [1–3] and have been adopted for many applications. However, the development of harmless lead-free piezoceramics has gained a great deal of attention because of the near future restriction on the lead-based materials due to the environmental issues.

In the past several years, much attention has been paid to the alkaline niobate-based materials, and especially to the potassium sodium niobate $K_{0.5}Na_{0.5}NbO_3$ (KNN) family. KNN is one of the most promising candidates for lead-free piezoelectric ceramics because of its high Curie temperature (about 420 ℃) and large electromechanical coupling factors [4,5]. However, the difficulty in sintering KNN under the atmospheric conditions is a serious drawback, and various techniques such as hot pressing and spark plasma sintering have been utilized in order to improve the sinterability of KNN ceramics [6,7]. Since these techniques are found unsuitable for use in industrial production, many sintering aids are researched by several researchers in order to sinter KNN under atmospheric conditions, such as $K_{5.4}Cu_{1.3}Ta_{10}O_{29}$, CuO and MnO_2 [8–15]. Nevertheless, the piezoelectric properties of the KNN system are degraded in these cases although these sintering aids can improve the sinterability of the KNN ceramics. Therefore, the novel

* Corresponding author.
E-mail: qiu@nuaa.edu.cn

sintering aids, which improve both the sintering behavior and piezoelectric properties, are key research.

Because $K_{5.70}Li_{4.07}Nb_{10.23}O_{30}$ (KLN) as aid has not been studied, the sintering behaviors and piezoelectric properties of KNN ceramics with KLN added are investigated by conventional sintering technique.

2 Experimental

A conventional ceramic fabrication technique was used to prepare $K_{0.5}Na_{0.5}NbO_3$–*x*mol%$K_{5.70}Li_{4.07}Nb_{10.23}O_{30}$ ($0 \leqslant x \leqslant 2.5$, KNN–*x*mol%KLN) ceramics using analytical-grade metal oxides or carbonate powders: K_2CO_3 (99%), Na_2CO_3 (99.8%), Li_2CO_3 (98%) and Nb_2O_5 (99.5%). The KNN and KLN powders were first synthesized at 900 ℃ for 5 h by a solid-state reaction method. After the calcination, KNN and KLN powders were weighted according to the formula of KNN–*x*mol%KLN and ball milled for 12 h. The resulting mixture was further mixed with polyvinyl alcohol binder solution thoroughly and then pressed into disk samples. The disk samples were sintered at 1100 ℃ for 2 h in air.

Density of the samples was determined by the Archimedes method. The crystalline phase was analyzed using an X-ray diffractometer (D8 Advance). The microstructure was observed by a scanning electron microscope (JSM-5610LV/Noran-Vantage). Dielectric properties as functions of temperature and frequency were measured by an impedance analyzer (HP4294A). Polarization vs. electric field hysteresis loops were measured using a ferroelectric test system (TF Analyzer 2000). Silver electrodes were fired on the top and bottom surfaces of the sintered samples. The ceramics were poled under a DC field of 2 kV/mm at 110 ℃ in a silicon oil bath for 30 min. The piezoelectric constant d_{33} was measured using a quasistatic piezoelectric constant testing meter (ZJ-3A, Institute of Acoustics, Chinese Academy of Sciences, Beijing, China).

3 Results and discussion

Figure 1 shows the X-ray diffraction (XRD) patterns of KNN–*x*mol%KLN ceramics. All of the ceramics exhibit single phase perovskite structure which indicates that excess Li^+ and K^+ may incorporate into the lattice. There are two peaks at about 45° which change obviously with different KLN contents. The

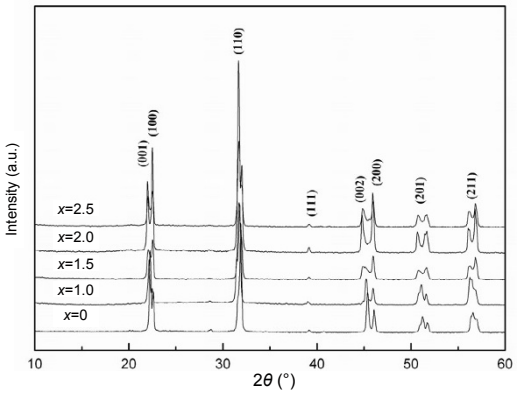

Fig. 1 XRD patterns of KNN–*x*mol%KLN ceramics with different KLN contents.

crystal structure can be distinguished from the relative intensity of these two peaks. For orthorhombic structure, the left peak at about 45° has higher intensity than that of the right peak, and it was indexed as (202) and (020), respectively. For tetragonal structure, the left peak at about 45° has lower intensity than that of the right peak, and it was indexed as (002) and (200), respectively. The phase structure of KNN–1mol%KLN is the orthorhombic structure while KNN–1.5mol%KLN exhibits tetragonal structure. Orthorhombic and tetragonal phases coexist in the ceramics when x is in the range of $1 < x < 1.5$.

The lattice parameters of KNN–*x*mol%KLN ceramics are calculated by fitting the diffraction peak profile, as shown in Fig. 2. Clearly, there is a transition zone between the orthorhombic and tetragonal phases in the range of $1 < x < 1.5$. When x is larger than 1.5, the materials become pure tetragonal phase. The tetragonality c/a is ~1.011 for KNN–1.5mol%KLN and increases to ~1.013 for the composition with $x = 2.5$.

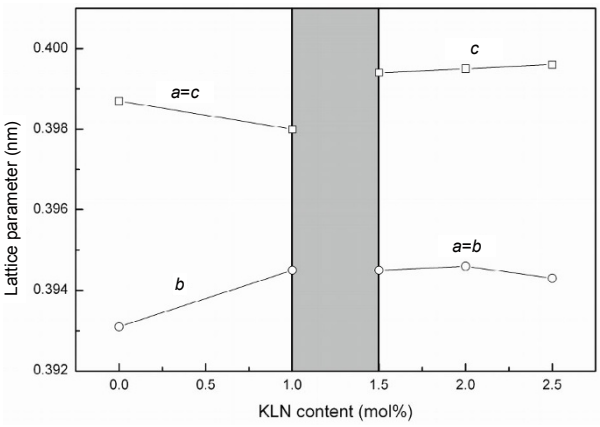

Fig. 2 Lattice parameters of KNN–*x*mol%KLN ceramics as a function of the KLN contents.

An increase in tetragonality usually corresponds to a rise in the Curie temperature for a couple of perovskite solid solution ceramics, such as $Pb(Zr,Ti)O_3$ [16].

Figure 3 shows the microstructures of KNN–*x*mol%KLN ceramics sintered at 1100 ℃. For the pure KNN ceramic (i.e., $x = 0$), the grains have a diameter in the range of 10 μm, and small amount of pores are observed (Figs. 3(a) and 3(b)). By the increasing x to 1, the grains become larger and more nonuniform (Figs. 3(c) and 3(d)). The ceramics are denser and almost no pore is observed. These results clearly show that the addition of KLN can improve the sintering performance of the ceramics. The grain growth is inhibited and average grain size is decreased with increasing x to 1, while the amount of pores decreases. This result explains that the grains of the KNN–1mol%KLN sample grow sufficiently.

For the KNN–1mol%KLN ceramic sintered at 1100 ℃, the average grain size of matrix grains in Figs. 3(c) and 3(d) is 3 μm. However, some coarse grains (or areas), which are indexed by grains 1 and grains 2, are also observed. In particular, the extremely large grains with diameter up to 20–30 μm as indexed by grains 1, can be clearly seen in Fig. 3(d). Obviously, this is a kind of abnormal grain growth (AGG) behavior, whose characteristic is the formation of some exceptionally large grains in a matrix of fine grains [17–19]. However, it seems that the AGG in the present material is different from the classical AGG behavior reported by other authors [20,21], because the abnormal grains in this study are much more like finer matrix grains aggregated together probably due to the formation of a liquid phase [22,23]. Because K^+ incorporates into the lattice which gives rise to the relatively higher content of K in KNN–*x*mol%KLN samples, the solidus temperature of KNN decreases with increasing the content of KLN from phase diagram of the $KNbO_3$–$NaNbO_3$ system [24]. On the other hand, the amount and fluidity of liquid phase increase with increasing KLN at 1100 ℃. When the content of KLN increases to 1 mol%, the numbers of large grains apparently increase. Meanwhile, two kinds of large grains can be classified. The one is abnormal large grains indexed by grains 1, while the other one is normal large grains indexed by grains 2 in Figs. 3(c) and 3(d). Furthermore, by increasing x to 2, only normal grain growth (NGG) behavior takes place and no abnormal large grain is observed as shown in Figs. 3(g)–3(j).

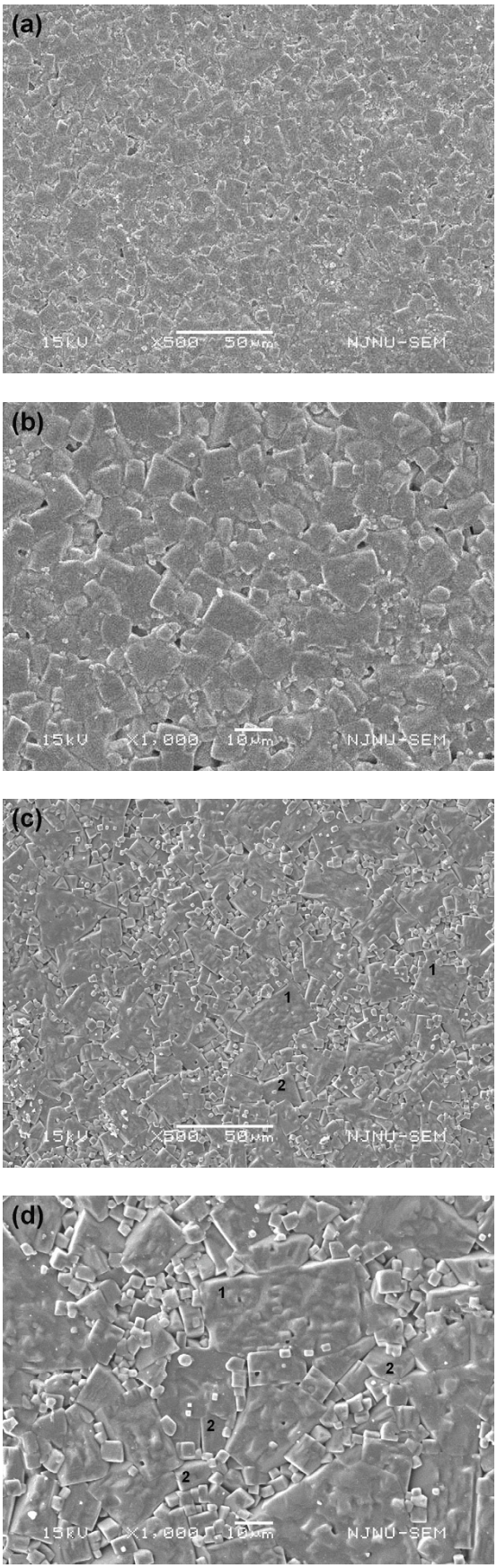

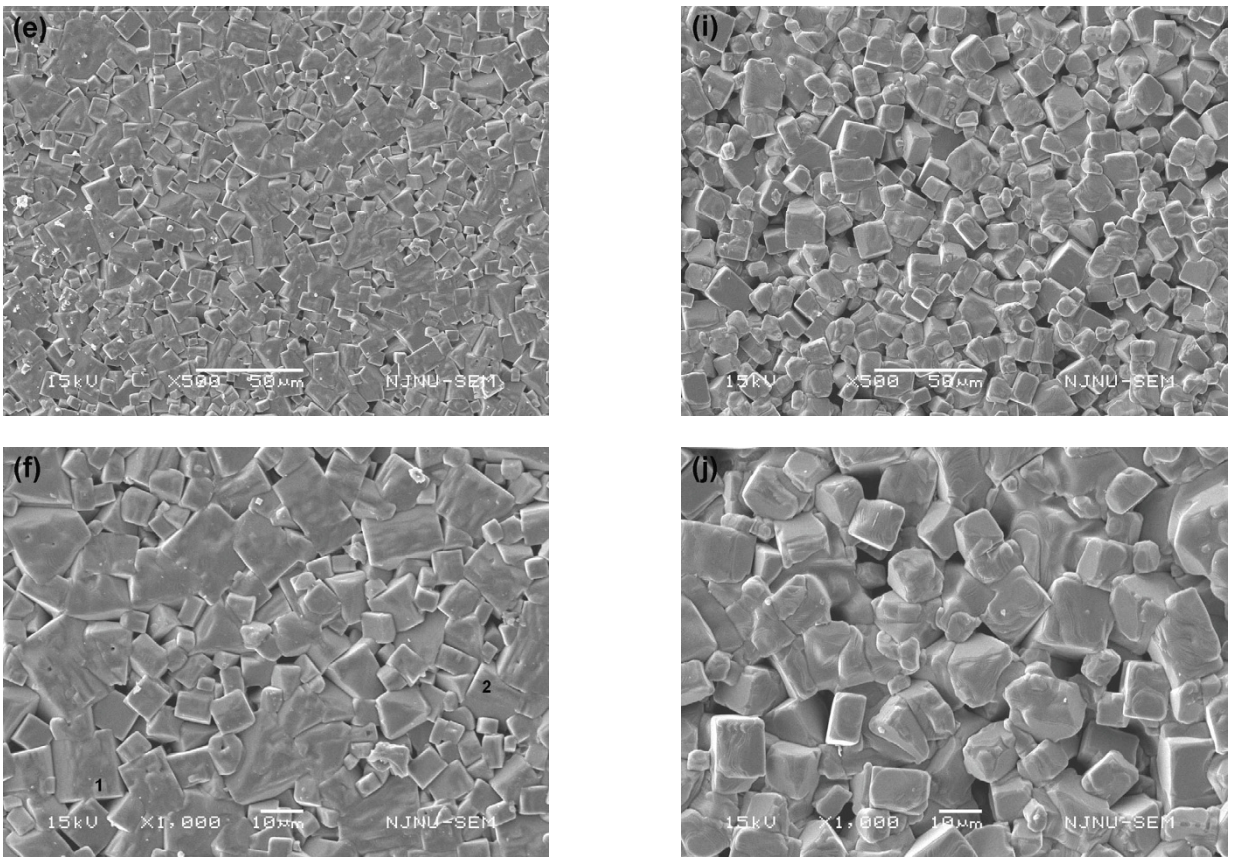

Fig. 3 SEM micrographs of KNN–*x*mol%KLN ceramics with various KLN contents: (a) and (b) $x = 0$; (c) and (d) $x = 1$; (e) and (f) $x = 1.5$; (g) and (h) $x = 2$; (i) and (j) $x = 2.5$.

On the basis of the microstructure evolution and our previous study on sintering aid, it is thought that AGG and NGG are related to the presence of a liquid phase. The formation mechanisms of a liquid phase in KNN and KNN-based ceramics have been just discussed. A small amount of liquid phases may form at first in some local areas probably when the content of KLN is 1 mol%, and the liquid phase amount in different local areas may be nonuniform owing to low fluidity and volatilization of alkali metal ions [25]. Based on the powder sintering theory [26], the grain growth is controlled by dissolution and precipitation mechanisms for the more amount of liquid phase, while it is controlled by diffusion for the less one. Therefore, classical large grains are observed in the local areas where the amount of liquid phase is more. Because of less liquid phase amount in the other areas, the small grains can not dissolve and become self-organized to be aligned into clusters, as can be seen in Fig. 3(d) where the small grains obey a discipline of controlled alignment by diffusion. Generally, a liquid phase

contributes to sintering by accelerating particle redistribution because of the enhanced high atom mobility. Besides, similar to the organic additives that accelerate transformation as the surfactants, liquid phase is supposed to act as a kind of surfactant during sintering at high temperature [22]. Also, the volatilization of alkali metal oxides in KNN-based ceramics might play a specific role in the microstructure formation [25]. Thus, the self-assembly of aggregation can be aided through a combined action of small grain surfactant interactions. Another positive effect of a liquid phase on the sintering is enhancement of the final sample density via a high capillary force. Figure 4 is a schematic showing how the AGG structure of a coarse grain is formed. As shown in Fig. 4, when the less liquid phase appears, the small grains distribute randomly and some small holes are even not eliminated. As the sintering time increases, the surfactant-mediated interactions accelerate the formation of self-assembled clusters by small grains. However, when the sintering time further increases, several groups of clusters with small disorientations are supposed to be bounded together to form coarse clusters. According to the classical grain growth [26], the grain growth rate is strongly dependent on the differences in grain radius and disorientation angles with the surrounding grains. For the small grains in the inner cluster structure, the grain boundary driving force is too small to move the boundary migration due to their small disorientations. Therefore, the small grains in the inner cluster structure have almost no growth, as shown in Fig. 3(d). Because of the more amount and higher fluidity of liquid phase, the matrix is easily filled and the proportion of NGG is improved with increasing KLN as shown in Figs. 3(e) and 3(f). When the liquid phase amount exceeds a certain value, the grain growth is controlled by dissolution and precipitation mechanisms, so AGG completely disappears.

Figure 5 shows the density and property variations of KNN–*x*mol%KLN ceramics sintered at 1100 ℃ for 2 h. As shown in Fig. 5, it has been observed that the KNN ceramic without KLN has a lower bulk density. The density of the KNN–*x*mol%KLN samples increases when the content of KLN increases from 0 to 1 mol%, and then slightly decreases when the content of KLN is above 1 mol%. Proper amount of KLN modification can increase the piezoelectric properties markedly. The d_{33} and k_p for KNN–1mol%KLN are 121 pC/N and 0.39, respectively. The significant enhancement in the piezoelectric properties results from the increase of bulk density and the phase structure of KNN–1mol%KLN which is around the polymorphic phase transition of the orthorhombic and tetragonal phases, as shown in Fig. 1. The polymorphic phase transition causes the higher piezoelectric activity owing to the more possible polarization states resulting from the coexistence of the orthorhombic and tetragonal phases. For $x>1$, d_{33} and k_p decrease probably because lower density with the increasing content of KLN. The Q_m value of KNN–*x*mol%KLN ceramics is enhanced with increasing KLN within the compositional range of KLN from 0 to 1 mol%. The highest Q_m value of 68 is achieved in the KNN–1mol%KLN ceramic. Q_m might be related to domain motion difficulty. The decrease in Q_m value is caused by the low density and the excess addition of KLN. As shown in Fig. 5, ε_r increases with increasing

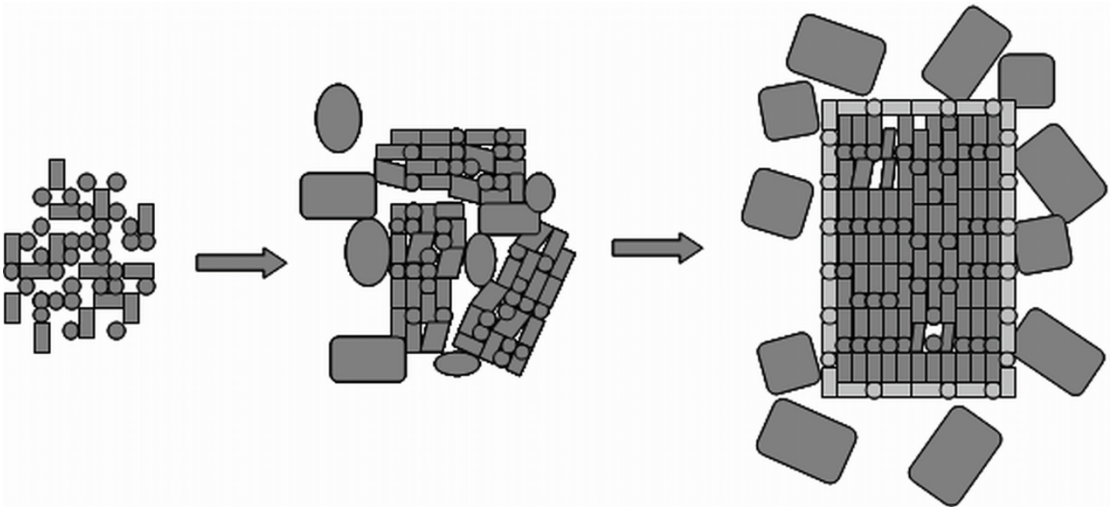

Fig. 4 Schematic diagram showing the formation procedure of AGG.

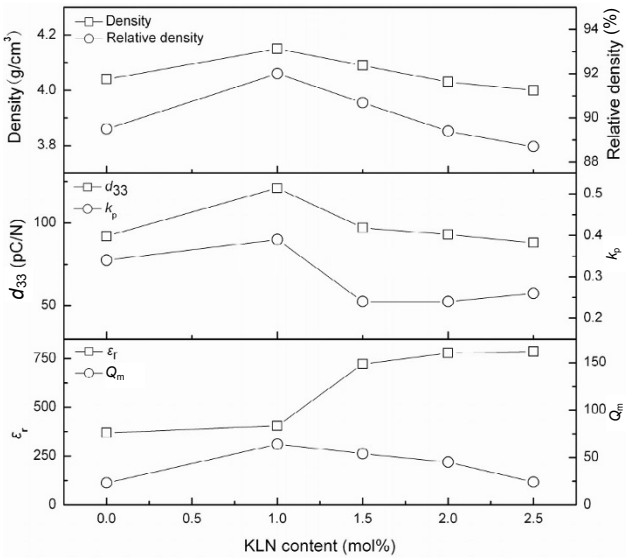

Fig. 5 Density, d_{33}, k_p, ε_r and Q_m values of the KNN–*x*mol%KLN ceramics with $0 \leqslant x \leqslant 2.5$.

KLN. These results confirm that the properties of KNN–1mol%KLN ceramic become optimum. The sample with $x = 1.0$ exhibits good properties: d_{33}, k_p, ε_r and Q_m show their peak values of 121 pC/N, 39%, 404 and 64, respectively.

Figure 6 shows the temperature dependence of dielectric constant ε_r (at 1 kHz) for KNN–*x*mol%KLN ($x = 0$, 1.5, 2.5) ceramics, and the inset shows the low temperature ferroelectric–ferroelectric transition (T_{O-T}). With the increase of KLN, the T_C increases and the maximum dielectric constant at T_C decreases. The ferroelectric–ferroelectric phase transition shifts to lower temperature, and the peak is slightly broadened which shows a diffusive nature with the increase of KLN. T_{O-T} is near room temperature at $x = 1.5$. When the content of KLN increases, Li^+ and K^+ could be incorporated into the lattice and compensate the volatilization of K^+ [25], so T_C increases. According to previous results [27,28], the incorporation of Li^+ will also cause the increase of T_C and decrease of T_{O-T}.

Figure 7 shows the *P*–*E* hysteresis loops of KNN–*x*mol%KLN ceramics. The P_r and E_C values for pure KNN ceramic are 6.36 μC/cm^2 and 1.26 kV/mm, respectively. Proper amount of KLN modification increases the remnant polarization and decreases the coercive field. It should be noted that the remnant polarization increases by 140% but the coercive field decreases by 24% when $x = 1$ ($P_r = 15.21$ μC/cm^2, $E_C = 0.957$ kV/mm). There are some mechanisms which are related to the increase of polarization and decrease of coercive field: the incorporation of Li^+ and the

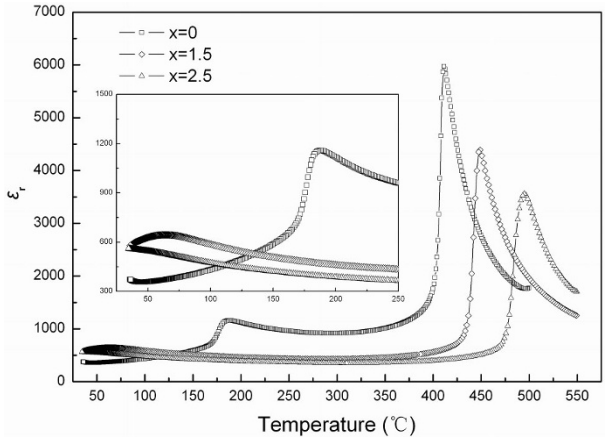

Fig. 6 Temperature dependence of dielectric constant ε_r for KNN–*x*mol%KLN ceramics.

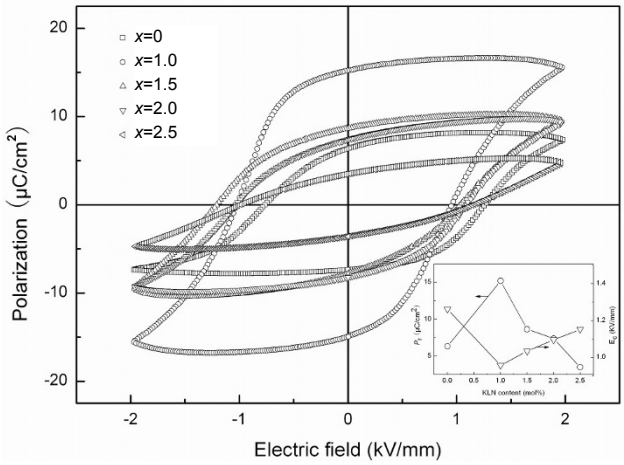

Fig. 7 *P*–*E* hysteresis loops of KNN–*x*mol%KLN ceramics.

decrease of defects. Li^+ has smaller ionic radius than K^+ and will cause the tilting of the Nb–O octahedron which increases the remnant polarization. The decrease of coercive field is mainly attributed to the decrease of the amount of defects. It is well-known that K_2O is volatile and K^+ vacancies will be left after sintering. The K^+ in KLN can compensate these vacancies and the amount of defects decreases. After $x \geqslant 1$, P_r decreases and E_C increases due to low density and poor microstructure as shown in Figs. 3(e)–3(j).

4 Conclusions

KNN–*x*mol%KLN ceramics were prepared by the solid-state reaction method. The results show that the small amount of KLN ($0 \leqslant x \leqslant 2.5$) incorporates into the lattice and forms the single phase perovskite

structure. It exhibits the polymorphic phase transition from orthorhombic structure to tetragonal structure when the content of KLN increases from 1 mol% to 1.5 mol%. The KNN–1mol%KLN ceramic shows AGG behavior. However, when the amount of KLN is increased above 1.5 mol%, abnormally grown grains disappear and relatively uniform microstructure with normally grown grains is formed. The AGG and NGG behaviors should be related to the volatilization of alkali metal oxides and the presence of liquid phase amount under different amount of KLN. KLN modification lowers T_{O-T} and increases T_C with increase of x. KNN–1mol%KLN ceramic shows a very high remnant polarization and low coercive field, and its piezoelectric properties are also the best among them.

Acknowledgements

This work was supported by the Natural Science Foundation of Jiangsu Province, China (BK20130791), Projects of International Cooperation and Exchanges NSFC (51161120326), Aeronautical Science Fund (20131552025), the NUAA Fundamental Research Funds (NS2013008), and a project funded by the Priority Academic Program Development of Jiangsu Higher Education Institutions (PAPD).

References

[1] Jaffe B, Roth RS, Marzullo S. Piezoelectric properties of lead zirconate–lead titanate solid–solution ceramics. *J Appl Phys* 1954, **25**: 809–810.

[2] Park S-E, Shrout TR. Ultrahigh strain and piezoelectric behavior in relaxor based ferroelectric single crystals. *J Appl Phys* 1997, **82**: 1804–1811.

[3] Fan H, Kim H-E. Effect of lead content on the structure and electrical properties of $Pb((Zn_{1/3}Nb_{2/3})_{0.5}(Zr_{0.47}Ti_{0.53})_{0.5})O_3$ ceramics. *J Am Ceram Soc* 2001, **84**: 636–638.

[4] Egerton L, Dillom DM. Piezoelectric and dielectric properties of ceramics in the system potassium–sodium niobate. *J Am Ceram Soc* 1959, **42**: 438–442.

[5] Zuo R, Fang X, Ye C. Phase structures and electrical properties of new lead-free $(Na_{0.5}K_{0.5})NbO_3$–$(Bi_{0.5}Na_{0.5})TiO_3$ ceramics. *Appl Phys Lett* 2007, **90**: 092904.

[6] Haertling GH. Properties of hot-pressed ferroelectric alkali niobate ceramics. *J Am Ceram Soc* 1967, **50**: 329–330.

[7] Wang R, Xie R, Sekiya T, *et al*. Piezoelectric properties of spark-plasma-sintered $(Na_{0.5}K_{0.5})NbO_3$–$PbTiO_3$ ceramics. *Jpn J Appl Phys* 2002, **41**: 7119–7122.

[8] Matsubara M, Kikuta K, Hirano S. Piezoelectric properties of $(K_{0.5}Na_{0.5})(Nb_{1-x}Ta_x)O_3$–$K_{5.4}CuTa_{10}O_{29}$ ceramics. *J Appl Phys* 2005, **97**: 114105.

[9] Takao H, Saito Y, Aoki Y, *et al*. Microstructural evolution of crystalline-oriented $(K_{0.5}Na_{0.5})NbO_3$ piezoelectric ceramics with a sintering aid of CuO. *J Am Ceram Soc* 2006, **89**: 1951–1956.

[10] Yang M-R, Hong C-S, Tsai C-C, *et al*. Effect of sintering temperature on the piezoelectric and ferroelectric characteristics of CuO doped $0.95(Na_{0.5}K_{0.5})NbO_3$–$0.05LiTaO_3$ ceramics. *J Alloys Compd* 2009, **488**: 169–173.

[11] Park S-H, Ahn C-W, Nahm S, *et al*. Microstructure and piezoelectric properties of ZnO-added $(Na_{0.5}K_{0.5})NbO_3$ ceramics. *Jpn J Appl Phys* 2004, **43**: L1072–L1074.

[12] Kosec M, Kolar D. On activated sintering and electrical properties of $NaKNbO_3$. *Mater Res Bull* 1975, **10**: 335–339.

[13] Tashiro S, Nagamatsu H, Nagata K. Sinterability and piezoelectric properties of $KNbO_3$ ceramics after substituting Pb and Na for K. *Jpn J Appl Phys* 2002, **41**: 7113–7118.

[14] Guo Y, Kakimoto K, Ohsato H. Dielectric and piezoelectric properties of lead-free $(Na_{0.5}K_{0.5})NbO_3$–$SrTiO_3$ ceramics. *Solid State Commun* 2004, **129**: 279–284.

[15] Kakimoto K, Masuda I, Ohsato H. Ferroelectric and piezoelectric properties of $KNbO_3$ ceramics containing small amounts of $LaFeO_3$. *Jpn J Appl Phys* 2003, **42**: 6102–6105.

[16] Choi SW, Shrout TR, Jang SJ, *et al*. Morphotropic phase boundary in $Pb(Mg_{1/3}Nb_{2/3})O_3$–$PbTiO_3$ system. *Mater Lett* 1989, **8**: 253–255.

[17] Kim M-S, Lee D-S, Park E-C, *et al*. Effect of Na_2O additions on the sinterability and piezoelectric properties of lead-free $95(Na_{0.5}K_{0.5})NbO_3$–$5LiTaO_3$ ceramics. *J Eur Ceram Soc* 2007, **27**: 4121–4124.

[18] Choi S-Y, Kang S-JL. Sintering kinetics by structural transition at grain boundaries in barium titanate. *Acta Mater* 2004, **52**: 2937–2943.

[19] Kim M-S, Jeong S-J, Song J-S. Microstructures and

piezoelectric properties in the Li_2O-excess $0.95(Na_{0.5}K_{0.5})NbO_3$–$0.05LiTaO_3$ ceramics. *J Am Ceram Soc* 2007, **90**: 3338–3340.

[20] Park CW, Yoon DY. Abnormal grain growth in alumina with anorthite liquid and the effect of MgO addition. *J Am Ceram Soc* 2002, **85**: 1585–1593.

[21] Kim M-S, Fisher JG, Kang S-JL, *et al*. Grain growth control and solid-state crystal growth by Li_2O/PbO addition and dislocation introduction in the PMN–35PT system. *J Am Ceram Soc* 2006, **89**: 1237–1243.

[22] Li J-F, Wang K, Zhang B-P, *et al*. Ferroelectric and piezoelectric properties of fine-grained $Na_{0.5}K_{0.5}NbO_3$ lead-free piezoelectric ceramics prepared by spark plasma sintering. *J Am Ceram Soc* 2006, **89**: 706–709.

[23] Zhen Y, Li J-F. Abnormal grain growth and new core–shell structure in $(K,Na)NbO_3$-based lead-free piezoelectric ceramics. *J Am Ceram Soc* 2007, **90**: 3496–3502.

[24] Ringgaard E, Wurlitzer T. Lead-free piezoceramics based on alkali niobates. *J Eur Ceram Soc* 2005, **25**: 2701–2706.

[25] Zhao P, Zhang B-P, Li J-F. High piezoelectric d_{33} coefficient in Li-modified lead-free $(Na,K)NbO_3$ ceramics sintered at optimal temperature. *Appl Phys Lett* 2007, **90**: 242909.

[26] Guo SJ. *Powder Sintering Theory*. Beijing: Metallurgical Industry Press, 1998.

[27] Guo Y, Kakimoto K, Ohsato H. Phase transitional behavior and piezoelectric properties of $(Na_{0.5}K_{0.5})NbO_3$–$LiNbO_3$ ceramics. *Appl Phys Lett* 2004, **85**: 4121–4123.

[28] Hollenstein E, Davis M, Damjanovic D, *et al*. Piezoelectric properties of Li- and Ta-modified $(K_{0.5}Na_{0.5})NbO_3$ ceramics. *Appl Phys Lett* 2005, **87**: 182905.